A Comparison of Energy Flows and Particle Spectra in Deep-Inelastic Scattering at HERA with Monte Carlo Models

G. Grindhammer[a], D. Krücker[b], and G. Nellen[a]

[a] Max-Planck-Institut für Physik, (Werner-Heisenberg-Institut), München, Germany
[b] Institut für Physik, Humboldt-Universität, Berlin, Germany

Abstract: Deep-inelastic scattering data taken at the ep-collider HERA on transverse energy flows and transverse momentum and pseudo-rapidity spectra of charged particles over a large range in the photon virtuality Q^2 and Bjorken x are compared to predictions from the Monte Carlo models ARIADNE, HERWIG, LEPTO, and RAPGAP.

1 Introduction

Recently comprehensive measurements of the transverse energy flow in deep-inelastic scattering (DIS) [1] have become available. They cover the kinematic range in Q^2, the photon virtuality, from about 3 to 2200 GeV^2, in the Bjorken scaling variable x from 8×10^{-5} to 0.11, and in the hadronic mass W from 66 to 233 GeV. When the high Q^2 part of that data were shown for the first time [2], none of the models then gave a satisfactory description of the data. In addition, there are data on transverse momentum and pseudo-rapidity spectra of charged particles [3]. These older data, however, cover only the low Q^2 region from 5 to 50 GeV^2, in x from 1.6×10^{-4} to 4.4×10^{-3}, and in W from 90 to 212 GeV.

We will use these data and compare them to four different Monte Carlo (MC) event generators based on the theory of Quantum Chromodynamics (QCD). The effect of recent modifications, where available, or of different options will be shown. It is not our aim here to tune parameters of the MC programs. It appears that the development of the programs has not sufficiently advanced yet to do that, particularly, if one demands that the high Q^2 and x and the low Q^2 and x kinematic regions are both well described simultaneously [4].

2 Monte Carlo models

We consider four different MC models, ARIADNE [5], HERWIG [6], LEPTO [7], and RAPGAP [8].

They all use phenomenologically derived parton density functions (PDFS) for the proton and in some cases for the photon, evolved to the relevant scale. The evolution of the parton cascade is performed backwards. We speak of a direct process, when the virtual photon itself interacts directly with a parton from the proton. This parton is then evolved backwards to the proton. In contrast to a direct process, a resolved process is one where a parton from the photon interacts with a parton from the proton. In this situation two space-like parton cascades may develop, one as before back to the proton and another one back to the photon. If a hard scattering occurs, the cross section for it is calculated using leading order (LO) QCD. The final state partons at this stage may then undergo further time-like parton showers until their virtuality has become sufficiently small to be fragmented into observable hadrons.

The PDFS of the proton are well constrained by inclusive measurements of DIS and by data from hadron-hadron colliders. The effects of using different PDFS within the limits allowed by the F_2 DIS measurements are small compared to the effects arising from other aspects of the simulation. For all MC simulations we have used here the LO CTEQ4L [9, 10] parametrisation. In addition, we have used in all programs the corresponding $\Lambda_{QCD} = 181$ MeV for four flavors together with the LO formula for the strong coupling parameter α_s. For simulations of resolved virtual photon processes, the LO SAS-G [11] virtual photon PDFS were used.

For the evolution of the parton cascade different equations are used. They have been derived in the leading-log approximation and are expected to be valid in certain regions of x and Q^2. The DGLAP [12] evolution equation effectively resums the leading $\ln Q^2$-terms, leading to strong ordering in transverse momentum of successive parton emissions, and is applicable at large Q^2. In the BFKL [13] approach leading $\ln(1/x)$-terms are resummed. In this case successive parton emissions are strongly ordered in longitudinal momentum but perform a random walk in transverse momentum. This latter feature is emulated by the colour dipole model (CDM) [14] in which gluons are radiated from colour dipoles.

Two different models, the string [15] and the cluster [16] model are available for the fragmentation of the final perturbative partons and the decays of the resulting primary hadrons.

The MC models used here are based on various combinations of the possible ingredients described above. They will be mentioned briefly below as well as changes to default settings and modifications of the programs. Another still short but useful account of most of the models can be found in [4].

2.1 ARIADNE 4.10

ARIADNE [5] is an implementation of the CDM [14], including corrections for the LO QCD matrix elements [17]. The default version 4.10 does not show any increase of the transverse energy with Q^2, in contrast to what is observed in the data [1]. A modification for DIS, reducing the phase space restriction due to the extended colour source of the proton remnant, was introduced to improve this behaviour [18]. In the figures, to be shown later, this is labeled with *new* hQ^2. In addition, simulations with two different sets of parameters [4], set 1 / set 2: $PARA(10) = 1.6/1.2$, $PARA(15) = 0.5/1.0$, and $PARA(25) = 1.4/0.$) are shown. The first two parameters govern the power of the soft suppression factor for gluon emission due to the colour extended proton remnant and struck quark [19], respectively. The third parameter influences the probability of having emissions outside the soft suppression cut-off. The corresponding distributions in the figures are labeled *set 99/1* and *set 99/2*. They include the modification for high Q^2.

2.2 LEPTO 6.5

LEPTO [7] matches LO QCD matrix elements to DGLAP based leading-log parton showers [20]. In addition, it allows for two different methods of non-perturbative rearrangement of the event colour topology via wee gluons which do not change the parton kinematics. The default option[1] for this version of LEPTO are the so called soft colour interactions (SCI) [21], where colour may be exchanged between the perturbatively produced final state partons of the event and the partonic proton remnant. This scheme allows to simulate rapidity gap events at HERA, however, it leads to an excess of soft particles at high Q^2 [22]. A new approach is based on string reinteractions according to a generalised area law (GAL) [23]. This allows interactions between two colour string pieces leading to a reduction in the total string area. Since this model is assumed to be universal, some retuned values of parameters[2] relating to hadronisation and the parton shower have to be used for this option. Distributions, shown in the figures, are for soft colour interactions on and off, labeled *SCI* and *no SCI* respectively, and for the GAL model, labeled *GAL*.

2.3 RAPGAP 2.06/48

Rapgap [8] is for direct photon DIS processes quite similar to LEPTO. In addition, it can simulate resolved photon processes. In order to be able to include resolved processes the scale $\mu^2 = \mu_r^2 = \mu_f^2$ has to be larger than Q^2. Here we have chosen $\mu^2 = p_T^2 + Q^2$ [24], where p_T is the transverse momentum of the jet. The effect on the direct contribution, compared to the choice $\mu^2 = Q^2$, is small. The default value for the p_T cut-off, needed to regulate the LO QCD matrix elements is $p_T^2 > PT2CUT = 1.0$ GeV^2. The contribution of the LO matrix element alone to the total cross section exceeds the measured DIS cross section if this cutoff is not sufficiently large. This has been the case for the default value at high Q^2. Therefore we have used $PT2CUT = 4.0$ GeV^2 everywhere.

For the fragmentation of the final perturbative partons into hadrons and their decays all of the above models use the string model [15] as implemented in JETSET 7.4 [25].

2.4 HERWIG 5.9

HERWIG [6] combines a coherent parton cascade with LO QCD matrix element corrections [26] and transforms the partons into hadrons using a cluster hadronisation model [16]. We have also used the perturbatively generated partons of HERWIG and fragmented them with the string model as implemented in JETSET. Ideally, one should then retune the fragmentation parameters, which we did not do. These simulations did not lead to a better description of the data and therefore we do not show any results. The default version of HERWIG implements the next-to-leading (NLO) running of the strong coupling parameter α_s. Here, we only use an implementation of the running of α_s in LO [27], which allows HERWIG to better follow the transverse energy flow data at high Q^2. A comparison to HERWIG with the running α_s in NLO can be found in [1]. In addition, we have used different settings of the parameters $CLMAX$, the maximum cluster mass parameter, and $PSPLT$, the parameter determining the splitting

[1]The LEPTO default includes the new sea-quark treatment with $LST(35) = 1$.

[2]The following parameters are used with the GAL option: $LST(34) = 3$, $PARJ(42) = 0.45$, $PARJ(82) = 2.0$, $PYPAR(22) = 4.0$, and $PARL(7) = 0.10$.

of clusters above mass $CLMAX$. The distributions shown are labeled α_s *LO* with the default settings of $CLMAX = 3.35$ and $PSPLT = 1.0$, *set 96* [28], *set 99/1*, and *set 99/2* [4] with $CLMAX = 5.5$, 3.0, 5.0 and $PSPLT = 0.65$, 1.2, 1.0 respectively.

3 Comparison with data

In order to compare data and predictions by the MC models, the data and utility package HzTool [29] has been used. In the following, in each figure the same corrected data are compared with all four models (see labels on the right hand side) separately. The error bars shown for the data include the statistical and systematic errors. All observables displayed in the figures have been calculated in the hadronic centre of mass[3] (HCMS).

In Fig. 1 the transverse energy flow [1] is shown as a function of the pseudo-rapidity, η^*, for four different bins, increasing in Q^2 and x, with the following mean values: $< Q^2 >= 3.2$ GeV^2, $< x >= 0.8 \times 10^{-4}$ for the left most bin, $< Q^2 >= 14.1$ GeV^2, $< x >= 0.63 \times 10^{-3}$, $< Q^2 >=$ 175 GeV^2, $< x >= 0.4 \times 10^{-2}$, and $< Q^2 >= 2200$ GeV^2, $< x >= 0.11$ for the right most bin. The data show a plateau in the current region ($\eta^* > 0$) at low Q^2, which becomes more peaked with increasing Q^2 with a significant increase of the E_T^*. This feature of the data is roughly described by all models. At the highest Q^2, the data are well described by ARIADNE for all options shown, all of which include the high Q^2 modification. LEPTO, at the highest Q^2, can describe the data without SCI or with GAL turned on. At the lowest Q^2, however, the data are not described when using the GAL approach to colour reconnections. RAPGAP at the highest Q^2 is consistently below the data, the remaining bins in Q^2 are reasonably well described; at the lowest Q^2, the additional resolved contribution improves the comparison slightly. All options of HERWIG shown agree well with the data at the highest Q^2, overall the parameter set 96 works best.

Fig. 2 compares the rise with Q^2 of the mean transverse energy in the central rapidity bin, $-0.5 < \eta^* < 0.5$, and in a bin associated with the photon fragmentation region, $2.0 < \eta^* < 3.0$, for the data [1] and for the models. All models predict a strong rise with Q^2 for the photon fragmentation region and a less strong rise for the central region, as observed in the data[4]. HERWIG with parameter set 96 gives a fair description of the data in the central rapidity region. The default and the sets 99/1 and 99/2 fail in this region, but describe the data more or less in the photon fragmentation region.

In Fig. 3 the transverse momentum spectra of charged particles in the rapidity interval, $0.5 < \eta^* < 1.5$, and for low Q^2 [3] are compared to the models. Three bins in Q^2 and x are shown, the left most bin with $< Q^2 >= 7$ GeV^2, $< x >= 1.6 \times 10^{-4}$, the middle bin with $< Q^2 >= 14$ GeV^2, $< x >= 0.64 \times 10^{-3}$, and the right most bin with $< Q^2 >= 32$ GeV^2, $< x >= 2.1 \times 10^{-3}$. While the highest Q^2 and x bin can be described by all models, only ARIADNE can describe the other two bins, indicating too little hard radiation in the other models. HERWIG with the new parameter sets 99/1 and 99/2 gives a much better description of the rise of the data at low p_T^* compared to set 96, but falls below the data at the highest p_T^*.

The charged particle multiplicities [3], for the same bins in Q^2 and x as before, are shown in Fig. 4 as a function of η^*. The direction of the proton remnant is to the left. All models can

[3]They are marked by a *.

[4]The apparent decrease of some of the MC curves at the highest Q^2 is an artifact, due to plotting curves instead of histogramms.

describe the highest Q^2 and x bin, LEPTO only with the no SCI or GAL option, and HERWIG only with set 99/2. ARIADNE and RAGAP succeed to describe the data in all bins. LEPTO can describe the lowest bin in Q^2 and x only with the no SCI option, and for HERWIG none of the presented options work well.

In Fig. 5 the charged particle multiplicities, but now only for particles with $p_T^* > 1$ GeV, are shown as a function η^*. Here only ARIADNE and HERWIG with set 96 and 99/2 are able to describe the data in all bins to some extent. All shown options of LEPTO and RAPGAP lie below the data for η^* in the direction of the proton remnant.

4 Summary

In general the models describe the DIS data on transverse energy flows, transverse momentum spectra, and pseudo-rapidity spectra of charged particles in the hadronic centre of mass better the larger Q^2 and x are. None of the models give a good description of the data over the whole range in Q^2 and x. For ARIADNE the modification of the phase space restriction for gluon emission is essential at large Q^2. All models, except for ARIADNE, fail to describe the high p_T tail of the charged particle spectra, particularly for particles in the direction towards the proton remnant, indicating too little hard parton radiation in the models. Taking this into account, it is perhaps not surprising that the soft colour reconnection models of LEPTO do not have enough impact in helping to describe for example the transverse energy flows. HERWIG also uses non-perturbative effects, which depend on how large in mass the remnant cluster is allowed to become, to increase or decrease the energy flow in the direction of the proton remnant. This also allows to improve the transverse momentum spectrum for intermediate transverse momenta, but fails to describe the hard perturbative tail seen in the data. Of all the models, ARIADNE provides the best description of the data.

References

[1] H1 Collab., C. Adloff et al., DESY 99-091, submitted to *Eur. Phys. J.* **C** , (1999).

[2] D. Krücker, in Proc. 3rd Workshop in Small-x and Diffractive Physics, Argonne (1996).

[3] H1 Collab., C. Adloff et al., *Nucl. Phys.* **B 485**, 3 (1997).

[4] N.H. Brook et al., 'A Comparison of Deep Inelastic Scattering Monte Carlo Event Generators to HERA Data', these proceedings and http://www.desy.de/~heramc.

[5] L. Lönnblad, *Comp. Phys. Commun.* **71**, 15 (1992).

[6] G. Marchesini et al., *Comp. Phys. Commun.* **67**, 465 (1992).

[7] G. Ingelman, A. Edin, J. Rathsman, *Comp. Phys. Commun.* **101**, 108 (1997).

[8] H. Jung, *Comp. Phys. Commun.* **86**, 147 (1995), http://www-h1.desy.de/~jung/rapgap.html.

[9] CTEQ Collab., H.L. Lai et al. *Phys. Rev.* **D 55**, 1280 (1997).

[10] H. Plothow-Besch, *PDFLIB Version 7.09, User's Manual, W5051 1997.07.2 CERN-PPE* (1997).

[11] G.A. Schuler and T. Sjöstrand, *Phys. Lett.* **B 376**, 193 (1996).

[12] V.N. Gribov and L.N. Lipatov, *Sov. J. Nucl. Phys.* **15**, 438 and 675 (1972);
G. Altarelli and G. Parisi, *Nucl. Phys.* **B 126**, 298 (1977);
Yu.L. Dokshitzer, *Sov. Phys. JETP* **46**, 641 (1977).

[13] E.A. Kuraev, L.N. Lipatov, and V.S. Fadin, *Sov. Phys. JETP* **45**, 199 (1977);
Ya.Ya. Balitsky and L.N. Lipatov, *Sov. J. Nucl. Phys.* **28**, 822 (1978).

[14] G. Gustafson, *Phys. Lett.* **B 175**, 453 (1986);
G. Gustafson and U. Petterson, *Nucl. Phys.* **B 306**, 746 (1988);
B. Andersson, G. Gustafson, L. Lönnblad, and U. Petterson, *Z. Phys.* **C 43**, 625 (1989).

[15] B. Andersson, G. Gustafson, G. Ingelman, and T. Sjöstrand, *Phys. Rep.* **9803**, 6 (1998).

[16] B.R. Webber, *Nucl. Phys.* **B 238**, 492 (1984);
G. Marchesini and B.R. Webber, *Nucl. Phys.* **B 310**, 461 (1988).

[17] L. Lönnblad, *Z. Phys.* **C 65**, 285 (1995).

[18] L. Lönnblad, 'The high Q^2 behaviour of ARIADNE', these proceedings.

[19] L. Lönnblad, M. Seymour, et al., Proc. Physics at LEP 2 Workshop, eds. G. Altarelli, T. Sjöstrand, and F. Zwirner, CERN/96-01, vol. 2, 187 (1996).

[20] M. Bengtsson and T. Sjöstrand, *Comp. Phys. Commun.* **37**, 465 (1988).

[21] A. Edin, G. Ingelman, and J. Rathsman, *Comp. Phys. Commun.* **75**, 57 (1997) and *Phys. Lett.* **B 366**, 371 (1996).

[22] ZEUS Collab., J. Breitweg et al., DESY 99-041, accepted by *Eur. Phys. J.* **C** , (1999).

[23] J. Rathsman, *Phys. Lett.* **B 452**, 364 (1999).

[24] H. Jung, L. Jönsson, and H. Küster, DESY 98-051, hep-ph/9805396.

[25] T. Sjöstrand, *Comp. Phys. Commun.* **39**, 347 (1986);
T. Sjöstrand and M. Bengtsson, *Comp. Phys. Commun.* **43**, 1987 (367);
T. Sjöstrand, *Comp. Phys. Commun.* **82**, 74 (1994).

[26] M.H. Seymour, *Nucl. Phys.* **B 436**, 443 (1995) and *Nucl. Phys.* **B 436**, 443 (1995).

[27] J. Chyla, H1 internal note.

[28] N.H. Brook et al., in Proc. 'Future Physics at HERA', Eds. G. Ingelman, A. De Roeck, R. Klanner, DESY 96-235, 613 (1996), http://www.desy.de/~heraws96.

[29] J. Bromley et al., in Proc. 'Future Physics at HERA', Eds. G. Ingelman, A. De Roeck, R. Klanner, DESY 96-235, 611 (1996), http://www.desy.de/~heraws96 and http://www.desy.de/~heramc/mclist.html.

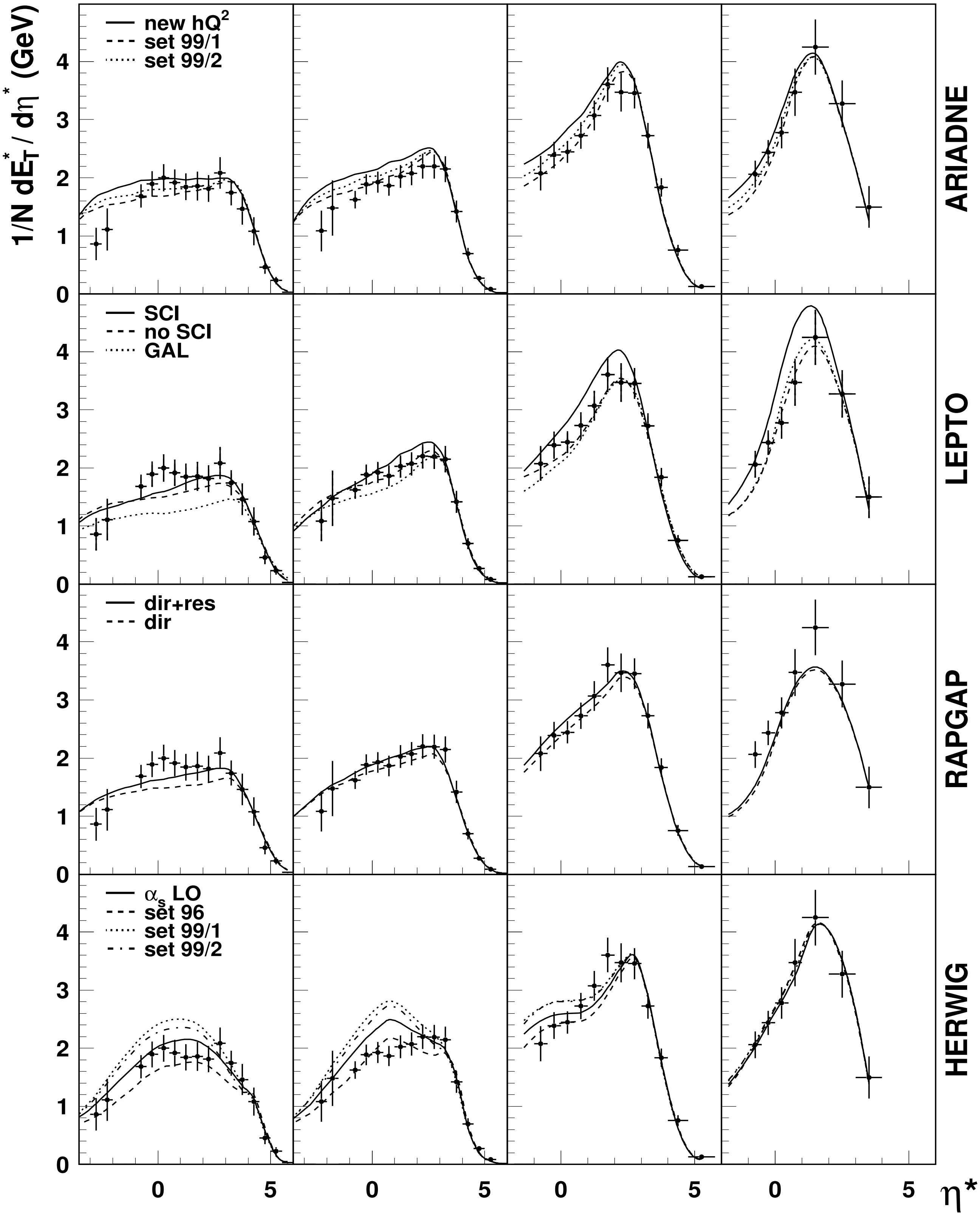

Figure 1: *The transverse energy flow, measured by H1 in the HCMS, compared to different MC model predictions. Four different DIS regions are shown. They are from left to right:* $< Q^2 >= 3.2\ GeV^2$, $< x >= 0.8 \times 10^{-4}$, $< Q^2 >= 14.1\ GeV^2$, $< x >= 0.63 \times 10^{-3}$, $< Q^2 >= 175\ GeV^2$, $< x >= 0.4 \times 10^{-2}$, *and* $< Q^2 >= 2200\ GeV^2$, $< x >= 0.11$.

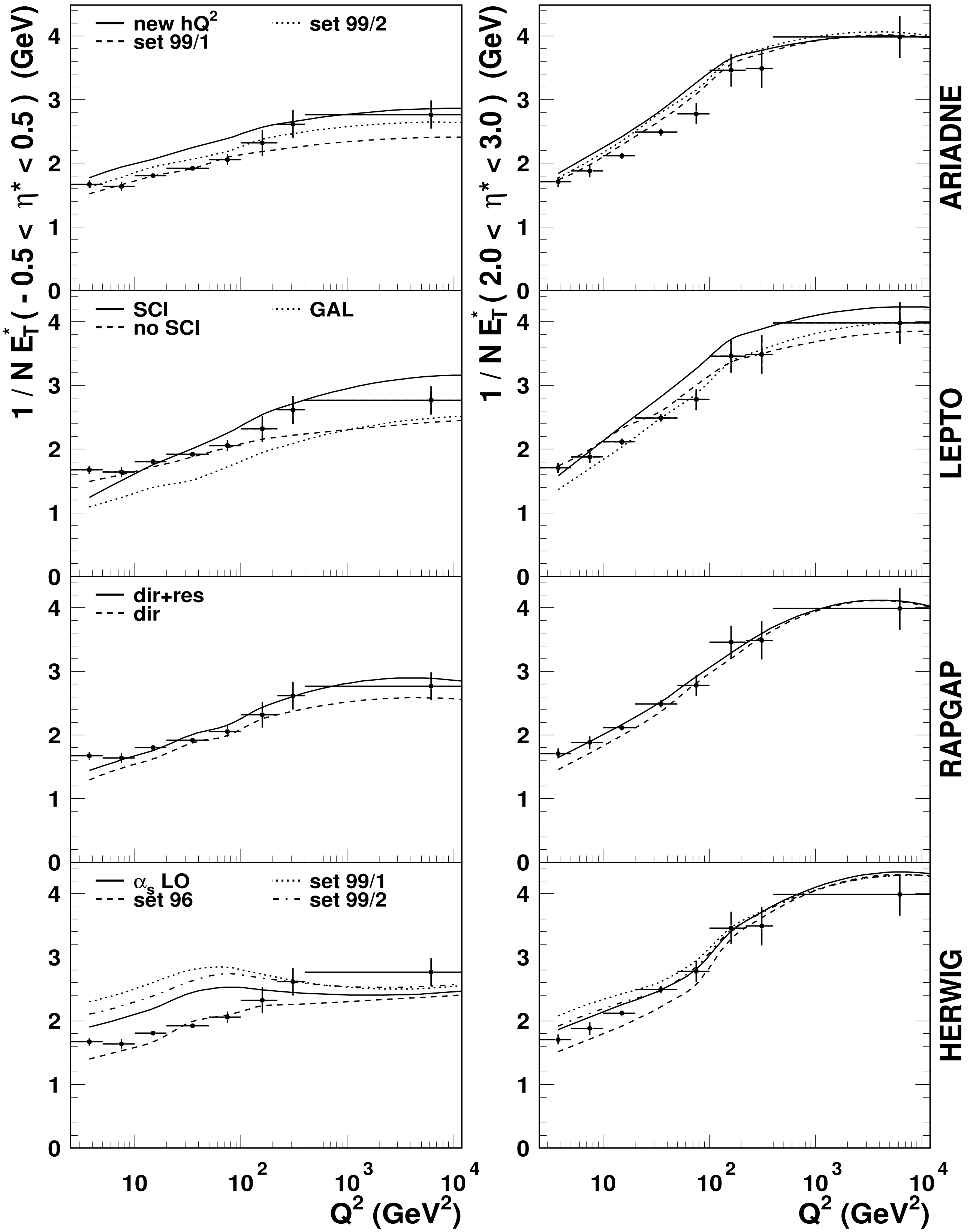

Figure 2: *The mean transverse energy, in the central region of pseudo-rapidity (left) and in the photon fragmentation region (right), measured by H1 in the HCMS, compared to different MC model predictions.*

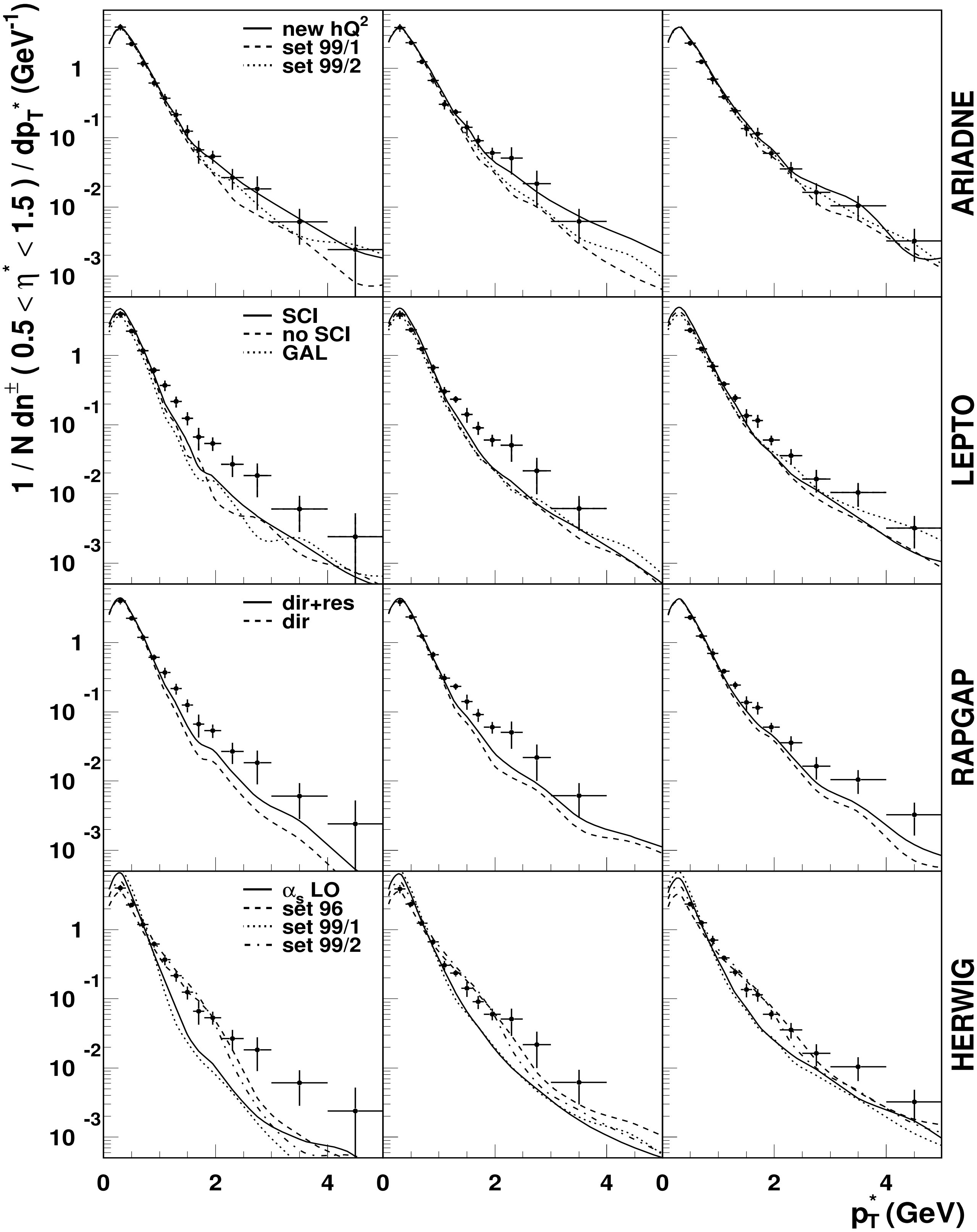

Figure 3: *The transverse momentum spectra of charged particles, measured by H1 in the HCMS in the pseudo-rapidity interval* $0.5 < \eta^* < 1.5$*, compared to different MC model predictions. Three different DIS regions are shown. They are from left to right:* $<Q^2>= 7\ GeV^2$, $<x>= 1.6\times10^{-4}$, $<Q^2>= 14\ GeV^2$, $<x>= 0.64\times10^{-3}$*, and* $<Q^2>= 32\ GeV^2$, $<x>= 2.1\times10^{-3}$.

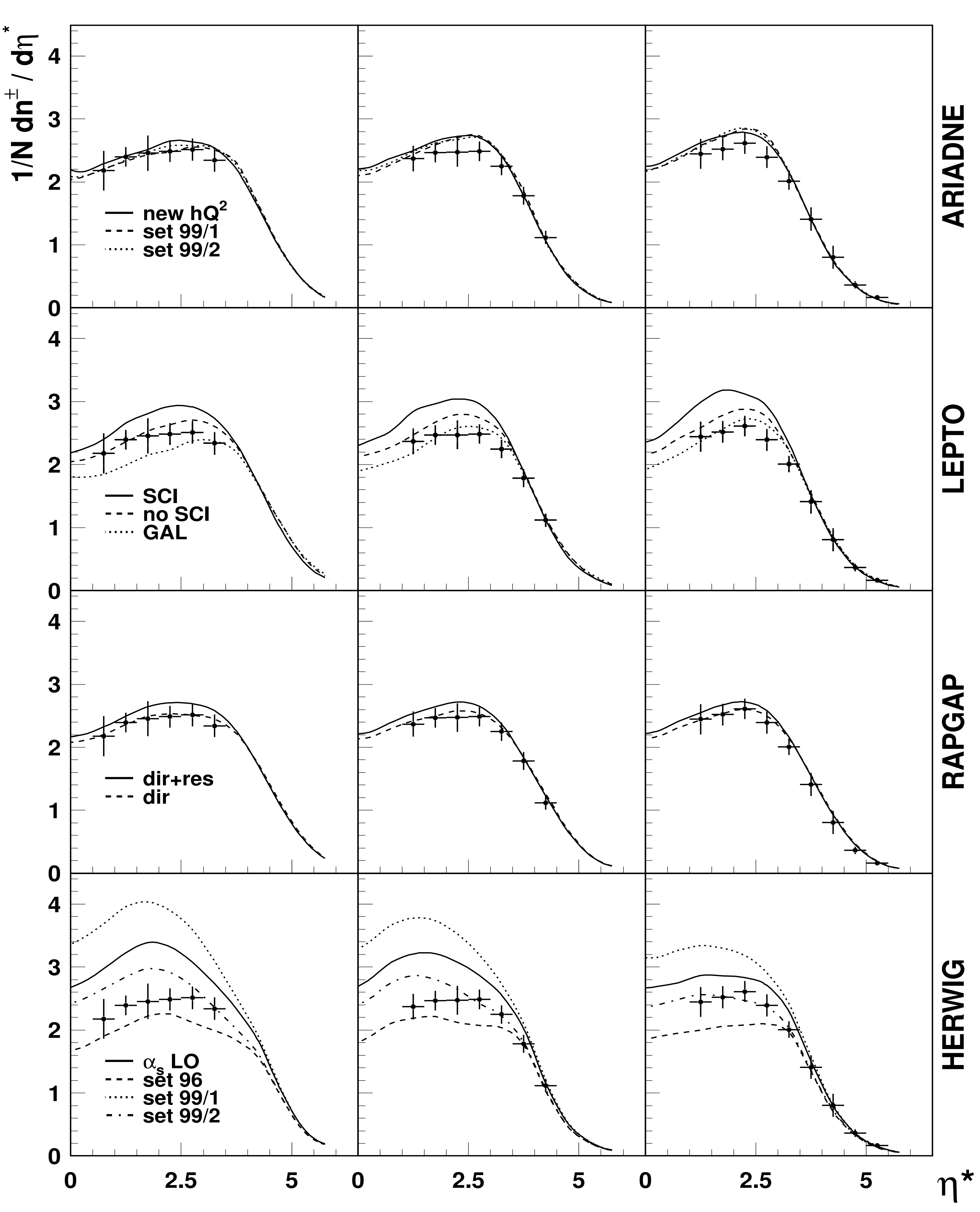

Figure 4: *The pseudo-rapidity spectra for charged particles, measured by H1 in the HCMS, compared to different MC model predictions. The direction of the photon remnant is to the left. Three different DIS regions are shown. They are from left to right:* $< Q^2 >= 7\ GeV^2$, $< x >= 1.6 \times 10^{-4}$, $< Q^2 >= 14\ GeV^2$, $< x >= 0.64 \times 10^{-3}$, *and* $< Q^2 >= 32\ GeV^2$, $< x >= 2.1 \times 10^{-3}$.

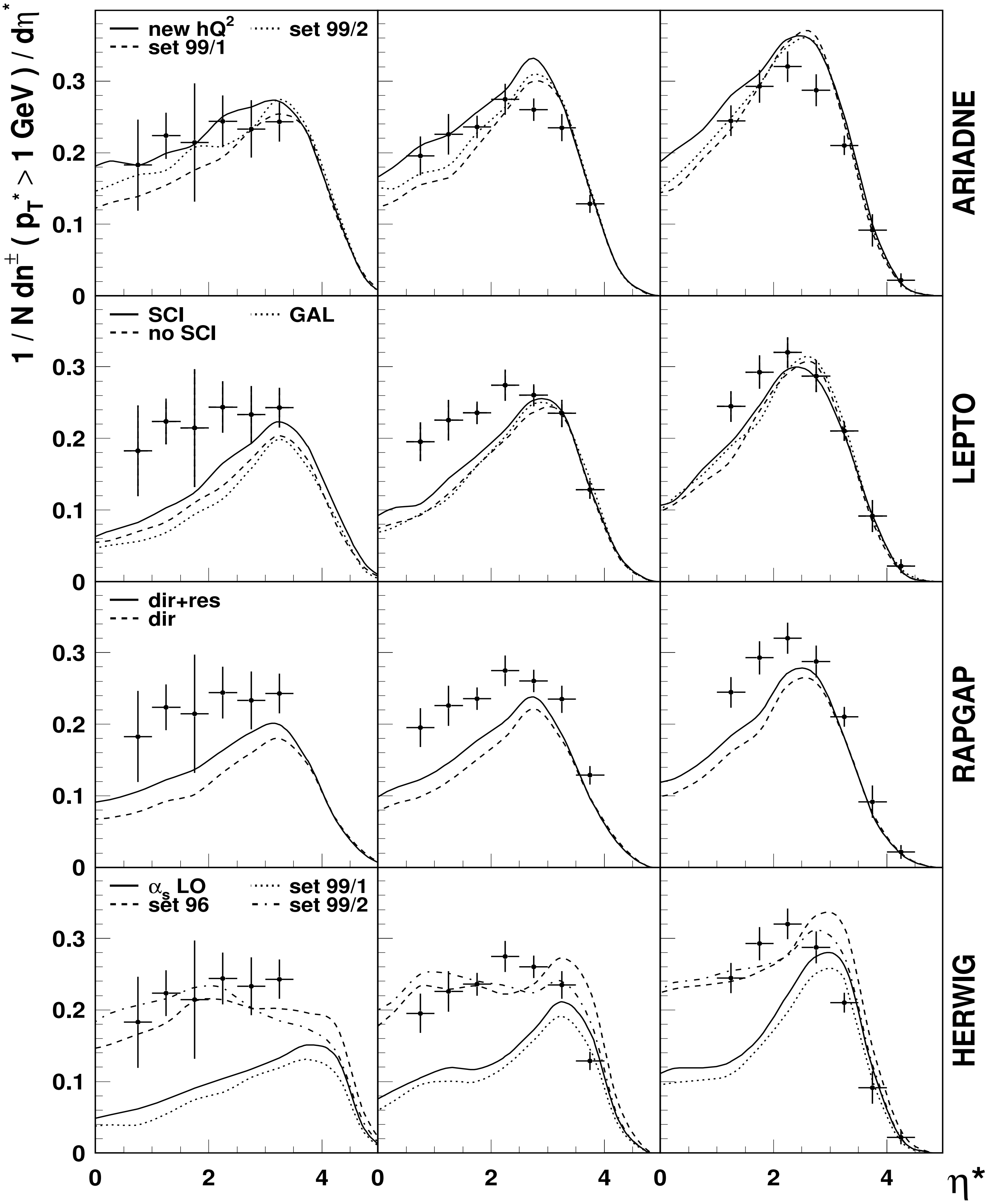

Figure 5: *The pseudo-rapidity spectra for charged particles with $p_T^* > 1$ GeV, measured by H1 in the HCMS, compared to different MC model predictions. The direction of the photon remnant is to the left. Three different DIS regions are shown. They are from left to right: $< Q^2 >= 7$ GeV^2, $< x >= 1.6 \times 10^{-4}$, $< Q^2 >= 14$ GeV^2, $< x >= 0.64 \times 10^{-3}$, and $< Q^2 >= 32$ GeV^2, $< x >= 2.1 \times 10^{-3}$.*